

Toward rapid silica analysis of CPDM samples: Deposition of recovered dust and analysis by FTIR

August Greth & Emily Sarver

To cite this article: August Greth & Emily Sarver (2025) Toward rapid silica analysis of CPDM samples: Deposition of recovered dust and analysis by FTIR, Journal of Occupational and Environmental Hygiene, 22:2, 87-100, DOI: [10.1080/15459624.2024.2421008](https://doi.org/10.1080/15459624.2024.2421008)

To link to this article: <https://doi.org/10.1080/15459624.2024.2421008>



View supplementary material [↗](#)



Published online: 10 Dec 2024.



Submit your article to this journal [↗](#)



Article views: 162



View related articles [↗](#)



View Crossmark data [↗](#)

REPORT



Toward rapid silica analysis of CPDM samples: Deposition of recovered dust and analysis by FTIR

August Greth and Emily Sarver

Department of Mining and Minerals Engineering, Virginia Polytechnic Institute & State University, Blacksburg, Virginia

ABSTRACT

The ongoing resurgence of severe Coal Workers' Pneumoconiosis in the US has been linked to overexposure to respirable crystalline silica (RCS, which is predominantly present as quartz and regulated as such). Capabilities that enable more frequent RCS monitoring are highly sought. Recent developments include field-based quartz analysis of traditional filter samples—collected on polyvinyl chloride (PVC) filters—using portable Fourier Transform Infrared spectroscopy (FTIR). However, most respirable dust samples in US coal mines are collected with a continuous personal dust monitor (CPDM) that enables real-time tracking of total respirable dust mass concentration. FTIR cannot directly analyze the collected dust sample due to the materials and construction of the sampling substrate. To address this issue, a simple three-step method was envisioned wherein the dust could be recovered into a suspension, redeposited onto a PVC filter using a syringe filter apparatus, and then analyzed by FTIR. The current study was conducted to develop the redeposition and analysis steps. It specifically considers the issues of the PVC filter size and deposition pattern yielded by typical filtration apparatuses and the FTIR scanning locations to establish a model that predicts quartz mass from the spectral data. Of the options tested here, the following combination was found to be optimal: 25-mm PVC filter with dust deposition using an inline syringe filter holder (which yields a “wheel and spoke” pattern), and FTIR analysis at four center-offset locations (90° apart, 8-mm from the center) from which the spectral data were averaged. Under these conditions, the predicted quartz mass on filters with respirable dust deposited from one of two geologic source materials (i.e., representing real coal mine silica sources) was observed to have a standard error of 0.011 mg (11 µg) for samples with an expected quartz mass of less than 0.150 mg (which equated to a total sample mass of less than about 1.5 mg). For samples with higher expected quartz masses, standard error increased, suggesting that dust deposition becomes less uniform with increasing total sample mass.

KEYWORDS



Continuous personal dust monitor; Fourier transform infrared spectroscopy; respirable coal mine dust; respirable crystalline silica

Introduction

It is well established that overexposure to respirable coal mine dust (RCMD) can lead to debilitating lung disease (Laney and Weissman 2014; Liu and Liu 2020), and dust containing significant respirable crystalline silica (RCS) can be particularly hazardous (Castranova and Vallyathan 2000). Since 1977, U.S. federal regulations have imposed a permissible exposure limit (PEL) on RCMD mass concentration (30 US Code of Federal Regulations, part 70); the regulations have also set limits on α -quartz content in RCMD (termed simply “quartz” from here), which is the predominant form of crystalline silica in coal mines

(Key-Schwartz et al. 2003). To demonstrate compliance with regulatory standards, RCMD sampling is conducted by mine operators and mine inspectors (i.e., from the U.S. Mine Safety and Health Administration, MSHA) following strict requirements regarding, among other conditions, sampling equipment and materials and sample analysis.

Following the implementation of federal RCMD regulations, the prevalence of Coal Workers' Pneumoconiosis (CWP, or “black lung”) among U.S. underground coal miners steadily decreased until the late 1990s—and then a startling resurgence began (NIOSH 2011). This new era of CWP is still ongoing. It is characterized by high rates of the most severe

CONTACT Emily Sarver  esarver@vt.edu  Department of Mining and Minerals Engineering, Virginia Polytechnic Institute & State University, Blacksburg, VA, USA.

 Supplemental data for this article can be accessed online at <https://doi.org/10.1080/15459624.2024.2421008>. AIHA and ACGIH members may also access supplementary material at <http://oeh.tandfonline.com>.

© 2024 JOEH, LLC

form of the disease, progressive massive fibrosis (PMF), especially among central Appalachian miners (Blackley et al. 2016, 2018; Hall et al. 2019a). There is mounting evidence that RCS exposures are a primary factor in the recent PMF surge (Hall et al. 2019b; Cohen et al. 2022).

RCMD sampling and monitoring in US mines

Between 1970 and 2016, all RCMD sampling in U.S. mines was done using coal mine dust personal sampler units (CMDPSUs). These use a small air pump and cyclone separator to collect the respirable fraction of the airborne dust (i.e., particles with aerodynamic diameter less than 10 μm , with about 50% of the 4 μm particles penetrating the cyclone) (Jacobson and Lamonic 1969; Kissell et al. 2002). The dust sample is deposited on a pre-weighed 37-mm polyvinyl chloride (PVC) filter housed within a closed cassette. Following sample collection, the filter is sent offsite for analysis. RCMD concentration is determined gravimetrically: the filter is post-weighed, such that sample mass can be determined by difference with the pre-weight; then RCMD concentration is defined as the ratio of the sample mass to total volume of air sampled (i.e., based on flow rate and sampling duration). To determine quartz content (mass percentage) in the RCMD, the standard MSHA Method P-7 is used: the filter is ashed to remove combustible content (i.e., coal and the filter itself); the residue is deposited for analysis by FTIR to determine the mass of quartz (as a proxy for RCS); then the quartz content is computed as a percentage of the RCMD mass (Goldberg et al. 1984; MSHA 1994).

In response to the resurgence of CWP in the late 1990s and 2000s, MSHA promulgated a “new dust rule” for underground coal mines in 2014 (MSHA 2014). In addition to lowering the RCMD exposure limit from 2.0 mg/m^3 to 1.5 mg/m^3 , the rule mandated the use of new equipment for some compliance sampling. As of 2016, when the new dust rules were fully implemented, typically only MSHA inspector-conducted sampling (required every quarter) used the CMDPSU—and the resultant filter samples continued to be sent to an analytical laboratory for Method P-7 analysis. However, for personal sampling that must be conducted by the mine operator, the use of a CPDM rather than the CMDPSU is now required. While the required frequency of mine operator sampling increased (from five to fifteen consecutive shifts per quarter for each occupation being sampled), the CPDM was only designed to monitor RCMD mass

concentration (Volkwein et al. 2002, 2004, 2005, 2006; Page et al. 2007; Volkwein 2008). As described below, it does not collect a filter sample that is compatible with Method P-7 or other standard analysis methods for RCS.

The only commercially available CPDM that is certified by MSHA as intrinsically safe for use in underground coal mines is the Thermo Scientific personal dust monitor (TPDM) (Waltham, Massachusetts, USA). Like the CMDPSU, the CPDM uses a cyclone to separate the respirable-sized particles from the total airborne dust. However, rather than collecting the dust onto a PVC filter for post hoc analysis, the CPDM deposits the dust onto a specially designed filter assembly that enables continuous mass measurements by a tapered-element oscillating microbalance (TEOM). The filter assembly consists of a woven borosilicate glass fiber filter bound to a 15-mm polypropylene (PP) stub with polytetrafluoroethylene (PTFE) (Tuchman et al. 2008; Chow et al. 2022). The stub is mounted to the narrow end of a tube and the wider end of the tube is fixed. As air passes through the filter and the tube, the tube oscillates, and the TEOM essentially correlates changes in oscillation frequency to the rate of dust deposition on the filter (Williams and Vinson 1986; Cantrell et al. 1996). This allows measurement of RCMD mass concentration in near-real time (and the unit displays a cumulative work-shift average exposure to the wearer), but the collected dust sample cannot be analyzed by Method P-7 due to the materials and construction of the filter stub assembly (Tuchman et al. 2008; Miller et al. 2015; Chow et al. 2022). Indeed, common practice is currently to dispose of CPDM samples after the instrument’s data has been successfully transmitted to MSHA.

Direct-on-filter RCS analysis by portable FTIR

As noted, MSHA Method P-7 has historically been used for analyzing RCS (as quartz) in RCMD collected using standard filter samples (i.e., with the CMDPSU). The method requires careful gravimetric analysis (i.e., to weigh the filter) and sample preparation (i.e., ashing and deposition of the residue) for FTIR analysis. It is therefore conducted in a centralized lab and the time from sampling to results can be days to weeks (NASEM 2018). To enable expedited results—ideally, at the end of the shift on which a sample is collected—the Mining Research Division of the National Institute for Occupational Safety and Health (NIOSH) has developed a direct-on-filter method using a

portable FTIR spectrometer (NIOSH 2022). It was originally envisioned as a solution for personal RCS monitoring in coal mines (Miller et al. 2012, 2013), and has been demonstrated for this application (Pampena et al. 2020; Stacey et al. 2022). Additionally, use in other applications (e.g., metal/non-metal mining and construction, for engineering and research studies) and for other analytes (i.e., kaolinite and calcite) has been explored (Cauda et al. 2014; Weakley et al. 2014; Cauda et al. 2016; Hart et al. 2018; Chien et al. 2020; Pokhrel et al. 2021, 2022; Osho et al. 2024).

The end-of-shift method was designed for use with RCMD samples collected onto PVC filters using standard CMDPSUs (NIOSH 2022). However, since the 2014 “new dust rule” mandated the use of CPDMs for mine operator-conducted personal RCMD monitoring, CMDPSU sampling has become very limited (or non-existent) aside from the quarterly inspector-conducted sampling for quartz analysis. Moreover, just as samples on the CPDM filter stub are not suitable for Method P-7 analysis, they are not suitable for the direct-on-filter FTIR method. The borosilicate glass fiber content of the filter precisely interferes with the spectral signature of the quartz target analyte in the dust sample itself, which has been demonstrated using both absorbance and diffuse reflectance FTIR (Miller et al. 2015). Effectively, this leads to an ironic situation where the state-of-the-art technology for RCMD monitoring (CPDM) yields a sample that is incompatible with state-of-the-art capability for rapid RCS analysis (direct-on-filter FTIR).

Toward rapid RCS analysis of CPDM samples

To better protect miners from RCS exposures, MSHA recently published a “new silica rule” (MSHA 2024). It applies to all US mining sectors and sets the permissible exposure limit for RCS (quartz)¹ at 50 µg/m³ for a full shift of work, computed as an 8-hr time-weighted average (TWA), with an action level of 25 µg/m³ (i.e., above which additional RCS monitoring and corrective action by the mine operator is required). For coal mines, compliance sampling for RCS will still be done using the CMDPSU, and quartz analysis will still be performed by MSHA Method P-7. The sampling frequency will be determined by where initial results fall concerning the PEL and action level

but should be at least every 6 months. Separately, RCMD sampling will also continue as required by MSHAs 2014 “new dust rule”—meaning relatively frequently and with the CPDM.

While RCS compliance sampling and analysis must adhere to the regulatory requirements, the capability for non-regulatory analysis of CPDM samples could be quite valuable (Chow et al. 2022). For example, this could allow mines to gain further, more frequent insights about RCS trends in their operations—either by making use of the CPDM samples they are currently collecting for RCMD monitoring compliance and then disposing, or by collecting additional CPDM samples to support engineering studies (e.g., of dust sources or controls). As discussed above, an alternative CPDM filter substrate would be needed to enable direct-on-filter RCS analysis by FTIR (Miller et al. 2015). However, another option might be to recover dust from the current CPDM filter assembly, deposit it onto a suitable substrate (e.g., PVC), and then complete the analysis by FTIR. Figure 1 presents a conceptual illustration, which could potentially be performed on-site with a portable FTIR spectrometer.

Although the three major steps shown in Figure 1 appear straightforward, each has key factors that must be addressed to develop a reliable method: For CPDM sample recovery (Step 1), a procedure must be established that promotes predictable recovery of the dust while limiting and/or accounting for any contamination from the CPDM filter assembly itself. For sample deposition (Step 2), a procedure and syringe filter holder must be identified to yield a repeatable deposition pattern on the filter that will be analyzed by FTIR. This is critical because the FTIR spectral data is generated from one or more small-diameter scans (e.g., 6-mm circle), and must be used to predict the quartz mass across the entire filter area. For FTIR analysis (Step 3), the specific scan location(s) must therefore be established, and a corresponding spectral peak area-to-mass calibration model must be constructed.

While a feasible method for FTIR analysis of CPDM samples following Figure 1 ultimately depends on the successful execution of all three steps, the scope of the current study is limited to Steps 2 and 3. These steps are necessarily intertwined because the scan locations and calibration model are directly related to the dust deposition pattern on the final PVC filter. Steps 2 and 3 are also important precursors to experiments related to Step 1 since these must be worked out to evaluate dust recovery and any interference from the CPDM filter assembly itself.

¹For U.S. coal mines, quartz exposures heretofore have not been directly regulated via a PEL. Rather, the quartz content (mass percentage) in RCMD is measured and the RCMD concentration is limited to achieve an effective quartz PEL of 100 µg/m³. The 2024 “new silica rule” directly limits quartz concentration using a PEL of 50 µg/m³.

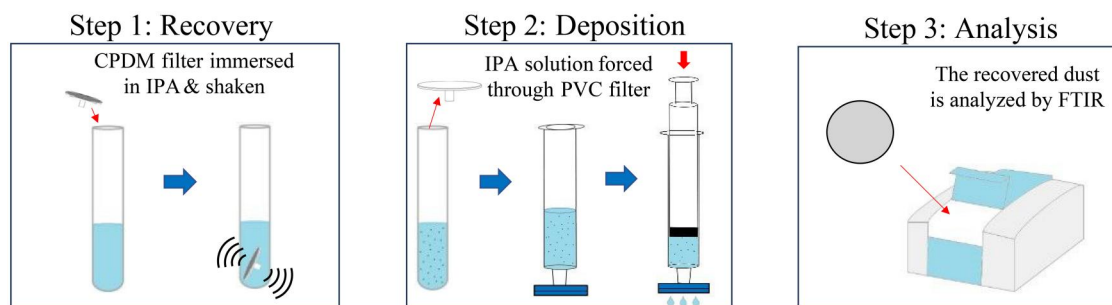


Figure 1. Conceptual illustration of a possible method to enable rapid RCS analysis of CPDM samples by FTIR.

Starting with a suspension of respirable-sized particles (i.e., to simulate dust recovered from a CPDM sample in Step 1), the specific objectives here are to: (1) test two candidate syringe-filter holders for depositing dust onto a PVC filter and (2) each filter holder, establish and evaluate quartz spectral peak area-to-mass calibration models for several FTIR scan location options.

Materials and methods

Dust source materials

As stated, the experimental work in the current study was designed to start with respirable particle suspensions to represent dust recovered from CPDM samples. For this, three materials were used. MIN-U-SIL 5 (US Silica, Katy, TX, USA) is a fine quartz product with a top size of 5 μm and median size of 1.6 μm , was used to generate particle suspensions for all tests to establish FTIR spectral peak area-to-mass calibration models. Additionally, two bulk samples of real coal mine dust source materials were used to generate particle suspensions for tests to evaluate the syringe-filter holder candidates and scan location options, and their corresponding calibration models. Both coal mine source materials were obtained from industry partners. One was taken directly from the dust collection system of a roof bolter, and the other was collected from raw roof rock material that was hand-picked from the mine production belt. The roof bolter material was very fine (i.e., dust generated during drilling and bolt installation), but the raw roof rock material had to be pulverized in the laboratory and sieved (to a product with a top size of about 60 μm) before collecting respirable dust particles.

To determine the mass percentage of quartz in the respirable fraction of all three dust source materials, samples were collected on 37-mm PVC filters (5 μm nominal pore size; Zefon International, Ocala, FL, USA) using standard CMDPSUs (see below). These samples were sent to a contract lab (RJ Lee Group,

Pittsburgh, PA, USA) for analysis by the standard NIOSH Method (NIOSH 2003), which is nearly identical to MSHA Method P-7. Results indicated the MIN-U-SIL 5 contained 91.7% quartz, which is consistent with results found in the literature (Stacey et al. 2009); and the bolter dust and the roof rock dust contained 9.52% and 10.5%, respectively.

Preparation of respirable dust suspensions

To prepare suspensions of respirable dust particles from each source material, the following procedure was used: A small quantity of the material was placed in a laboratory enclosure (measuring 35.6 \times 27.9 \times 40.6 cm) and aerosolized with compressed air. Respirable particles were sampled from the enclosure using a CMDPSU apparatus, which consisted of an air pump (Escort ELF; Zefon International, Ocala, FL, USA) operating at 2.0 L/min to pull the dust through a 10-mm Dorr-Oliver cyclone. The particles were collected onto 37-mm PTFE filters (nominal pore size 5 μm ; Zefon International, Ocala, FL, USA) in closed styrene cassettes; and filters were pre- and post-weighed using a Cubic MSE6.6S microbalance (Sartorius Corporation, Göttingen, Germany) and sample mass was estimated by simple difference. Notably, PTFE filters were chosen to collect the respirable particles at this stage due to their high collection efficiency; smooth surface, which enables high recovery of the particles into a suspension; and durability and chemical inertness, which minimizes contamination of the final dust suspension. In total, 60 samples of MIN-U-SIL and 70 samples of coal mine source materials (i.e., 36 from bolter dust and 34 from roof rock) were collected.

To prepare the respirable dust suspensions, each PTFE filter was placed in a clean PP test tube with approximately 6 mL of isopropyl alcohol (IPA) and sonicated for 3 min to dislodge the dust (per Greth et al. 2023; Greth et al. 2024). Then the PTFE filter

was removed, and the test tube was capped until the dust was deposited for FTIR analysis.

Dust deposition

Dust from each prepared suspension was deposited onto PVC filters (nominal 5 μm pore size; Zefon International, Ocala, FL, USA), either 25-mm or 13-mm diameter. The 25-mm filters were purchased pre-cut, however, the 13-mm filters were not available from the vendor so these were cut from 37-mm filters using a handheld hole punch. The deposition was conducted using a 50 mL Luer Lock syringe (BD, Franklin Lakes, NJ, USA) and one of two candidate filter holders: a 25-mm polypropylene plastic (PP) in-line filter holder, and a 13-mm stainless steel (SS) in-line filter holder (both from Sterlitech; Auburn, WA, USA). These two candidates were selected for testing considering several factors, including their wide availability, standard sizes, and compatibility with Luer Lok syringes. Additionally, though the direct-on-filter FTIR method for determining quartz content in RCMD has been developed using 37-mm filters (i.e., to be consistent with standard CMDPSU sampling), smaller filters are expected to be favorable for the envisioned method to analyze recovered CPDM samples. This is simply because the recovered dust should be more concentrated on a smaller filter area, which means smaller quartz masses can be detected and quantified. Another consideration was the filter support types that are included in the available filter holder options; this can influence the dust deposition pattern. Whereas plastic filter holders like the 25-mm PP option used here typically have a support structure with a “wheel and spoke” pattern, metal filter holders like the 13-mm option have a fine mesh as the filter support.

For the deposition procedure, each PVC filter was pre-weighed (using the same microbalance as above) and loaded into the appropriate filter holder. Then the filter holder was attached to a clean syringe, and one of the dust-in-IPA suspensions was transferred from its test tube to the syringe. The syringe plunger was carefully inserted and used to push the entire volume of the suspension through the filter. After removing the filter holder from the syringe, it was carefully opened, and the filter was allowed to dry completely in a clean fume hood. Finally, the filter was weighed again. Then, the expected quartz mass on the filter (Q_M , mg) was determined using Equation 1:

$$Q_M = (M_2 - M_1) \times Q_C \quad (1)$$

where M_1 and M_2 are the filter mass before and after dust deposition, respectively; and Q_C (%) is the quartz

content in the respirable dust collected from each source, as determined by NIOSH Method 7603.

Deposited dust analysis

Each PVC filter with deposited dust was analyzed by FTIR analysis a total of three times, with each analysis event on a different day. Notably, the first event directly followed the dust deposition and sample mass determination, and each filter was weighed again before the second and third analysis events (i.e., to enable evaluation of sample loss due to handling). The FTIR analysis was conducted with an $\alpha\alpha$ II FTIR portable spectrometer (Bruker Optics, Billerica, MA, USA) and associated OPUS software (Version 8.2.28). The instrument has a 6-mm diameter beam and measures the infrared absorbance of the sample between 4000 and 400 cm^{-1} . To analyze the filters, special square cassettes (one for the 25-mm filters and one for the 13-mm filters) were 3D-printed. The design was based on what NIOSH has designed for analysis of some 37-mm filters (NIOSH 2022). In essence, the filter is sandwiched securely between two square frames that have (aligned) circular openings that are just smaller than the filter diameter (i.e., to enable analysis anywhere on the filter except the edge). The overall cassette dimensions are such that the filter center is aligned with the center of the FTIR beam (6 mm in diameter). Additionally, to enable off-center analysis, “spacer” bars were printed with thicknesses of 2 mm and 4 mm; these can be placed under the square cassette to elevate it.

Since the FTIR spectrometer’s beam is much smaller than either the 13- or 25-mm filter area, the data must be effectively extrapolated to quantify quartz mass for the entire filter. While NIOSH (2022) has demonstrated that a single center scan is sufficient for direct analysis of airborne respirable dust collected on 37-mm filters, the current work is aimed at the analysis of dust that has been deposited from an IPA suspension using one of two syringe filter holders—and it was not known *a priori* if the deposit is predictably uniform. Thus, multiple scan locations were investigated here to identify combinations that may yield the most accurate results. As shown in Figure 2, each 25-mm PVC filter was analyzed in nine locations, namely the center (point 0), four 4-mm offset points (4A–4D), and four 8-mm offset points (8A–8D). For the offset points, one or two 4-mm spacer bars were placed under the square cassette to analyze the first point (A). Then, the square cassette was rotated 90° to analyze the next point (B), and the

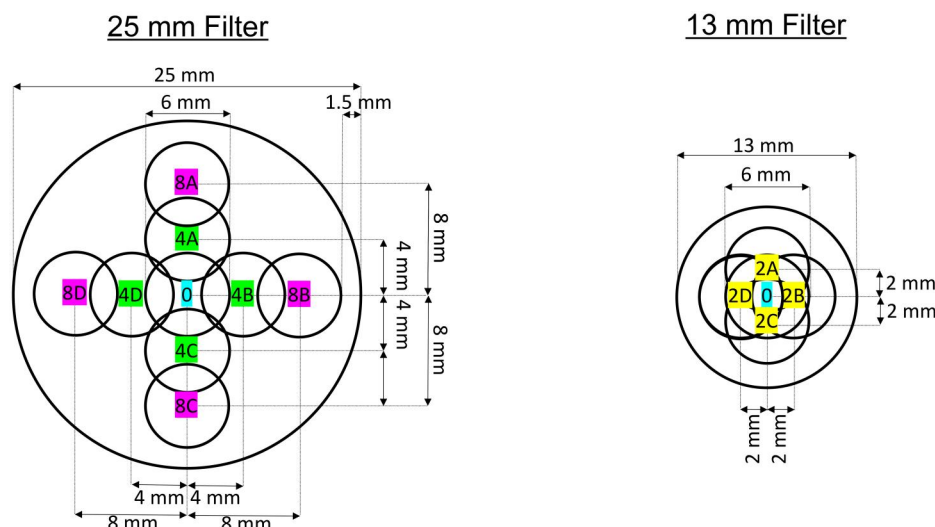


Figure 2. FTIR scan locations for 25-mm (left) and 13-mm (right) PVC filter samples with deposited dust from suspensions in IPA.

process was repeated for points C and D. For each 13-mm filter, analysis was conducted in five locations, namely the center, and at four 2-mm offset points (2A–2D) using a 2-mm spacer bar. For each analysis event, filters were analyzed in batches and, at the beginning of each batch, a new, blank PVC filter was analyzed at its center location to obtain data for blank corrections (i.e., to account for any interference from the PVC media itself, effects of humidity, etc.).

For the current study, each time a filter was analyzed, the instrument was set to perform 16 scans per scan location. The data were collected at 4 cm^{-1} resolution using the Blackman-Harris apodization, and then distortions were minimized using a rubber band baseline correction with 64 baseline points (Miller et al. 2017; NIOSH 2022). Next, the spectrum was blank-corrected to remove peaks associated with the PVC filter. Then, integrated spectral area (arbitrary units) was determined for two bands: $816\text{--}767\text{ cm}^{-1}$ corresponds to the band for the characteristic quartz doublet peak, and $930\text{--}890\text{ cm}^{-1}$ corresponds to the band for the primary kaolinite peak. While quartz is the target analyte, the kaolinite analysis is important because this mineral is commonly present in RCMD (Schatzel 2009; Su et al. 2020; Pokhrel et al. 2022) and it has a secondary peak (around 790 cm^{-1}) that interferes with the quartz analysis (Ojima 2003). However, because the two kaolinite peaks have integrated areas with a consistent ratio, the primary kaolinite peak area can be used to correct the quartz results for the interference caused by the secondary kaolinite peak. Per Miller et al. (2012), the corrected quartz peak area (QPA) can be determined by Equation 2:

$$\text{QPA} = \text{QPA}_{\text{uncorrected}} - \frac{\text{KPA}_1}{3.8} \quad (2)$$

where $\text{QPA}_{\text{uncorrected}}$ is the integrated quartz spectral peak area between 816 and 767 cm^{-1} , KPA_1 is the integrated primary kaolinite spectral peak area between 930 and 890 cm^{-1} , and 3.8 is the constant ratio assumed for the integrated areas under the primary and secondary kaolinite peaks. For each filter, a QPA value was determined for each scan location per analysis event.

Data analysis

Data from the filters with dust deposited from the MIN-U-SIL material were used to establish different QPA-to-mass calibration models by correlating observed QPAs (per Equation 2) with expected quartz mass (per Equation 1). The models differ by inclusion of data from specific scan locations (explained below). Then, the models were evaluated using the relevant data from the filters with dust deposited from the coal mine source materials. Correlation plots were created to compare predicted to expected quartz masses for each model, and model performance was evaluated based on standard error (SE) (i.e., between the predicted quartz mass values and a regression line).

To estimate limits of detection (LOD) and quantification (LOQ), data from 20 blank filters (of each size) were used. Each blank was analyzed by FTIR once using the same scan locations as for filters with deposited dust (i.e., per Figure 2), and QPA values were determined using Equation 2. Then, for each calibration model, LOD and LOQ were computed as $3\times$ and

10× the standard deviation, respectively, of the predicted quartz mass values observed for the blank filters (Lorberau 1990; Farcas et al. 2016; Chow et al. 2022).

Results and discussion

For each analysis event for each filter, the QPA per scan location and expected quartz mass are presented in the [Supplementary material: Tables S1 and S2](#) provide data for the 25-mm and 13-mm filters, respectively, with dust deposited from the MIN-U-SIL 5 material; and [Tables S3 and S4 \(Supplementary material\)](#) provide data for the 25-mm and 13-mm filters, respectively, with dust deposited from the coal mine source materials.

Establishing QPA-to-quartz mass calibration models

The filters with dust deposited from the MIN-U-SIL 5 material were used to establish QPA-to-quartz mass calibration models. For this, various combinations of the FTIR scan locations were considered per [Table 1](#): a total of eight combinations were considered for the 25-mm filters, and four combinations were considered for the 13-mm filters. The QPA values (given in [Supplementary material, Tables S1 or S2](#)) for the included scan locations were averaged per analysis event for every combination. E.g., for the 25-mm filter combination that consists of the center point plus all four 4 mm offset points (i.e., “Center + 4mm, 5-pt” in [Table 1](#)), the combined QPA was determined for each event as the average of QPAs observed from points 0, 4A, 4B, 4C, 4D in [Figure 2](#). Then, the per-event combined QPAs were averaged to yield a mean combined QPA (and standard deviation). To explore the possible effect of dissimilarity with groups of offset points, some combinations include only three of the four possible offset points at a given distance (e.g., the “4mm, 3 pt” model for 25-mm filters). For these

combinations, a sum-of-squared-differences approach was used to identify and exclude the point having a mean QPA value that was most dissimilar from the other three points’ values. Equations and example data for this approach are given in [Table S5 \(Supplementary material\)](#).

For each combination of the FTIR scan locations considered for the 25-mm and 13-mm filters, [Figure 3](#) presents correlation plots of the mean combined QPA values vs. the mean expected quartz mass on the filter. The error bars on each data point represent the standard deviation of mean values observed across the three analysis events. On each plot, the trendline shows a linear regression model fitted to the data, and the trendline equation and coefficient of determination (R^2) are shown. Notably, all trendline equations include a positive y-intercept, which indicates that the QPA is slightly higher than zero even when no quartz mass is expected. This is attributed, at least in part, to the influence of some higher-mass samples on the observed trends. However, minor interference from the IPA used to create the dust suspensions for this study could also be a factor; Ainsworth (2005) documented that IPA can interfere with quartz determination by FTIR if the alcohol has not completely evaporated. [Figure S1 \(Supplementary material\)](#) presents the same data shown in [Figure 3](#) except with regression models constrained such that the y-intercept is zero.

From [Figure 3](#), the relative magnitude of QPAs (and therefore regression line slopes) observed for the 25-mm filters is substantially lower than that of the 13-mm filters. This is because the dust deposit on the 13-mm filters is more concentrated. As evidenced by the narrow error bars associated with expected quartz mass data (i.e., x-axis error bars, related to sample weights before each FTIR analysis event), sample loss did not appear to be an issue even with three rounds of sample handling.

Regarding the 25-mm filters, [Figure 3](#) shows that the models associated with the center-offset scanning

Table 1. Combinations of FTIR scan locations on the 25-mm and 13-mm filters to establish QPA-to-quartz mass calibration models.

25-mm filter		13-mm filter	
Combination name	Location(s) on Filter	Combination name	Location(s) on Filter
Center	0	Center	0
4mm, 4-pt	4A, 4B, 4C, 4D	2 mm, 4-pt	2A, 2B, 2C, 2D
8mm, 4-pt	8A, 8B, 8C, 8D	Total, 5-pt	0, 2A, 2B, 2C, 2D
Total, 9-pt	0, 4A, 4B, 4C, 4D, 8A, 8B, 8C, 8D	2 mm, 3-pt	2A, 2B, 2C, 2D
Center + 4mm, 5-pt	0, 4A, 4B, 4C, 4D		
Center + 8mm, 5-pt	0, 8A, 8B, 8C, 8D		
4mm, 3-pt	4A, 4B, 4C, 4D		
8mm, 3-pt	8A, 8B, 8C, 8D		

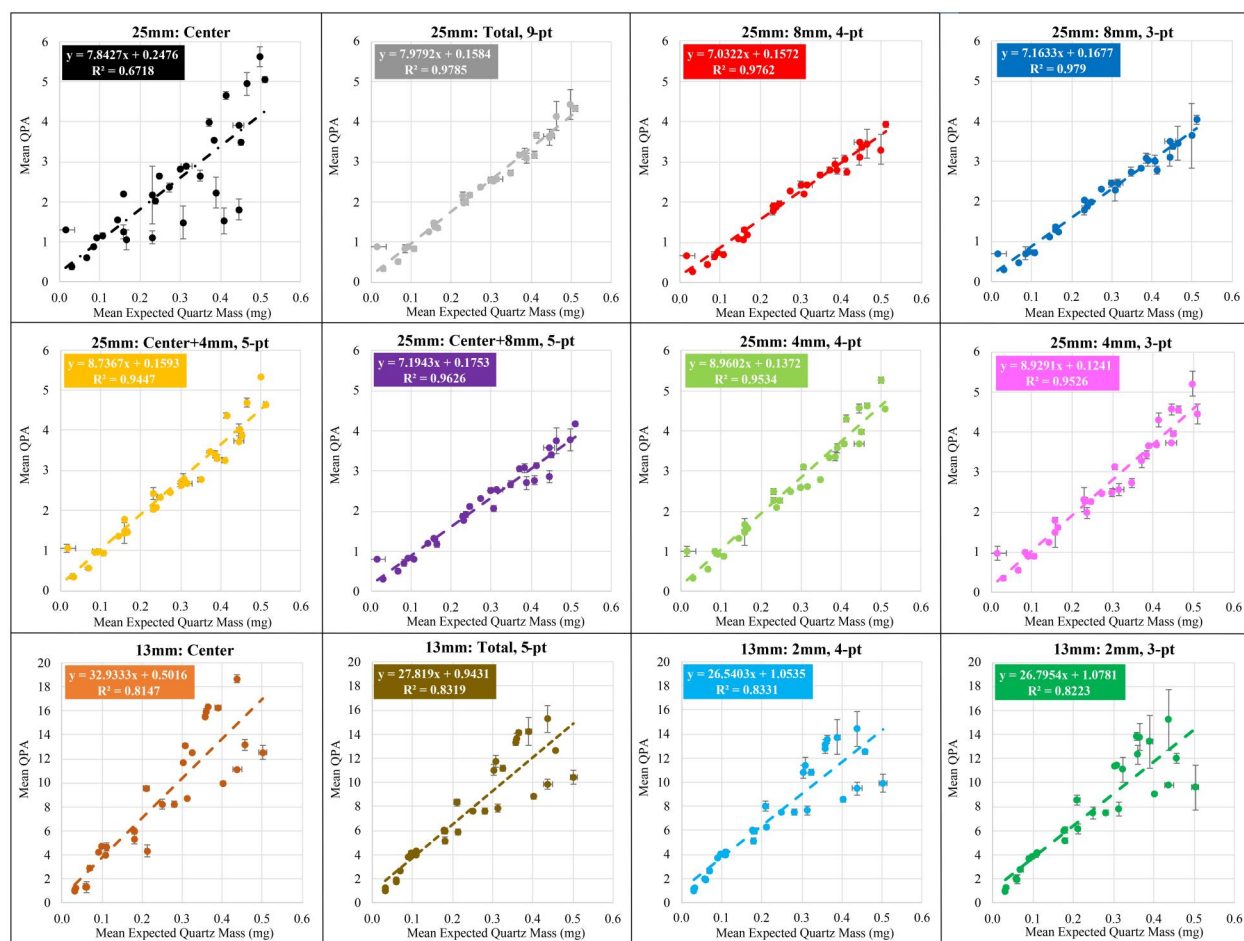
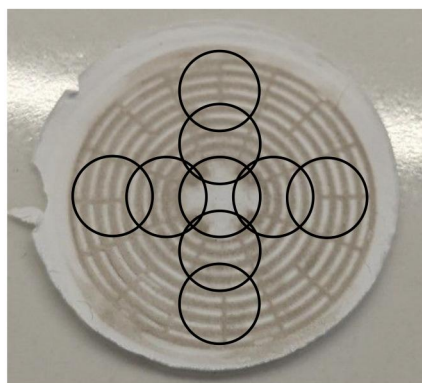


Figure 3. Correlation plots of mean combined QPA vs. mean expected quartz mass for filters with dust deposited from MIN-U-SIL 5 material. The top two rows show the eight data combinations considered for 25-mm filters ($n = 30$), and the bottom row shows the four combinations considered for 13-mm filters ($n = 30$).

25 mm Filter



13 mm Filter

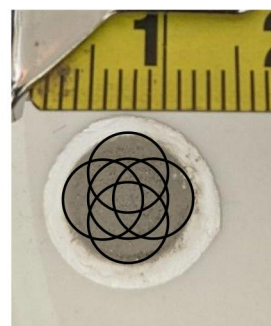


Figure 4. Photographs of the dust deposition pattern yielded by the 25-mm syringe filter holder (left) and the 13-mm syringe filter holder (right). On both photographs, the FTIR scan locations are overlaid for reference.

locations appear most promising. Overall, the data underlying these models show relatively little scatter, and generally small event-to-event variation (i.e., based on the narrow error bars around data points). The relative difference in the regression line slopes

between models dominated by 4-mm vs. 8-mm offset points is related to the specific “wheel and spoke” deposition pattern yielded by the filter support (see Figure 4) and indicates slightly higher loading (on average) at 4-mm vs. 8-mm; although R^2 values are

relatively high with either offset distance, especially when the center point is not included in the model.

On the other hand, the model established with only the center-point data appears to be the least favorable for the 25-mm filters, based on both scatter and the high event-to-event variability for numerous data points. The scatter is attributed to the deposition pattern, which includes a relatively large “blinded” area in the filter center (see [Figure 4](#)). Even a slight offset of the filter within the syringe filter holder could yield a difference in the ratio of loaded to blinded areas covered by the IR beam during a center scan—and this could cause scatter in the observed mean QPA to the expected quartz mass correlation. Moreover, slight differences in the filter alignment with the IR beam during separate analysis events (i.e., due to placement of the filter in the analysis cassette) could lead to variability in QPA values observed on a single filter.

For the 13-mm filters, [Figure 3](#) shows that data for all models have substantial scatter, and the “Center” model data also has relatively high event-to-event variation. In this case, the scatter is observed to trend with sample mass (i.e., more scatter for higher-mass samples). This could be related to some initial mass loss from samples where dust tended to “cake” on top of the filter during the deposition process—although, again, sample loss appears to have been relatively minor between analysis events. Another possibility is that a relatively thick dust deposit (i.e., for some higher-mass samples as exemplified in [Figure 4](#)) could have partially blocked the IR beam transmission. For the “Center” model data, the variation in QPA values between events might be related to the local non-uniformity of the dust deposit. Compared to the 25-mm filters, [Figure 4](#) does not show an obvious deposition pattern for the 13-mm filters, but the regression line slopes in [Figure 3](#) suggest the deposit was often center-heavy (i.e., the slope for the “center” only data is somewhat higher than slopes including only data collected at a 2-mm offset). Considering the geometry of the syringe (i.e., narrow outlet) and the filter holder (i.e., short distance between holder inlet and filter surface), it seems plausible that deposition uniformity should be the most variable in the filter center; in this location, deposition rate is initially expected to be greatest followed by flow rerouting to some extent as the filter loads. Combined with slight differences in the filter-IR beam alignment between analysis events, center-localized deposition non-uniformity could explain the event-to-event variation in center-derived QPA values.

Evaluating QPA-to-quartz mass calibration models

To evaluate the QPA-to-quartz mass calibration models established above, they were applied to predict quartz mass for each of the filters with dust deposited from the coal mine source materials. For this, the trendline equations shown in [Figure 3](#) were algebraically transformed to the form shown in [Equation 3](#):

$$x = \frac{y-b}{m} \quad (3)$$

where x is the predicted quartz mass (mg), y is the relevant combined QPA value, b is the y -intercept value, and m is the slope. Resultant model equations for all combinations considered in this study are given in [Table S6 \(Supplementary material\)](#), along with estimated LOD and LOQ values associated with each model. ([Supplementary material, Table S6](#) also shows the equations when y -intercept values were constrained to zero, i.e., per [Supplementary material, Figure S1](#).) For each filter, the relevant combined QPA values were used with each equation to predict quartz mass per analysis event, and then the mean predicted quartz mass (across all three events) was determined.

[Figure 5](#) compares the mean predicted quartz mass to the mean expected quartz mass for all filters with dust deposited from the coal mine source materials using all models. ([Supplementary material, Figure S2](#) presents the results using the model equations with y -intercept constrained to zero.) On each plot, a 1:1 reference line is shown along with a linear regression trendline. Like for [Figure 3](#), the error bars represent the standard deviation of mean values related to the three analysis events. In [Figure 5](#) (and [Supplementary material, Figure S2](#)), filters with dust from the roof rock and bolter dust are represented by different data markers. It is noted that, in general, the filters with dust deposited from the roof rock source material tended to have higher total sample mass, and thus higher expected quartz mass per [Equation 1](#). While the 25-mm filter data indicates, again, that sample loss between analysis events was generally minimal (i.e., narrow error bars in the x -axis direction), this was not the case for the 13-mm filters—and observations are discussed in more detail below.

[Figure 5](#) (and [Supplementary material, Figure S2](#)) demonstrates that quartz mass predictions made with QPA values from center-offset scan locations on the 25-mm filters are generally better than those made with the center-only scan data. This is evident from the observed trendline slopes, minimal y -intercept values, and relatively limited scatter of the data, and it is

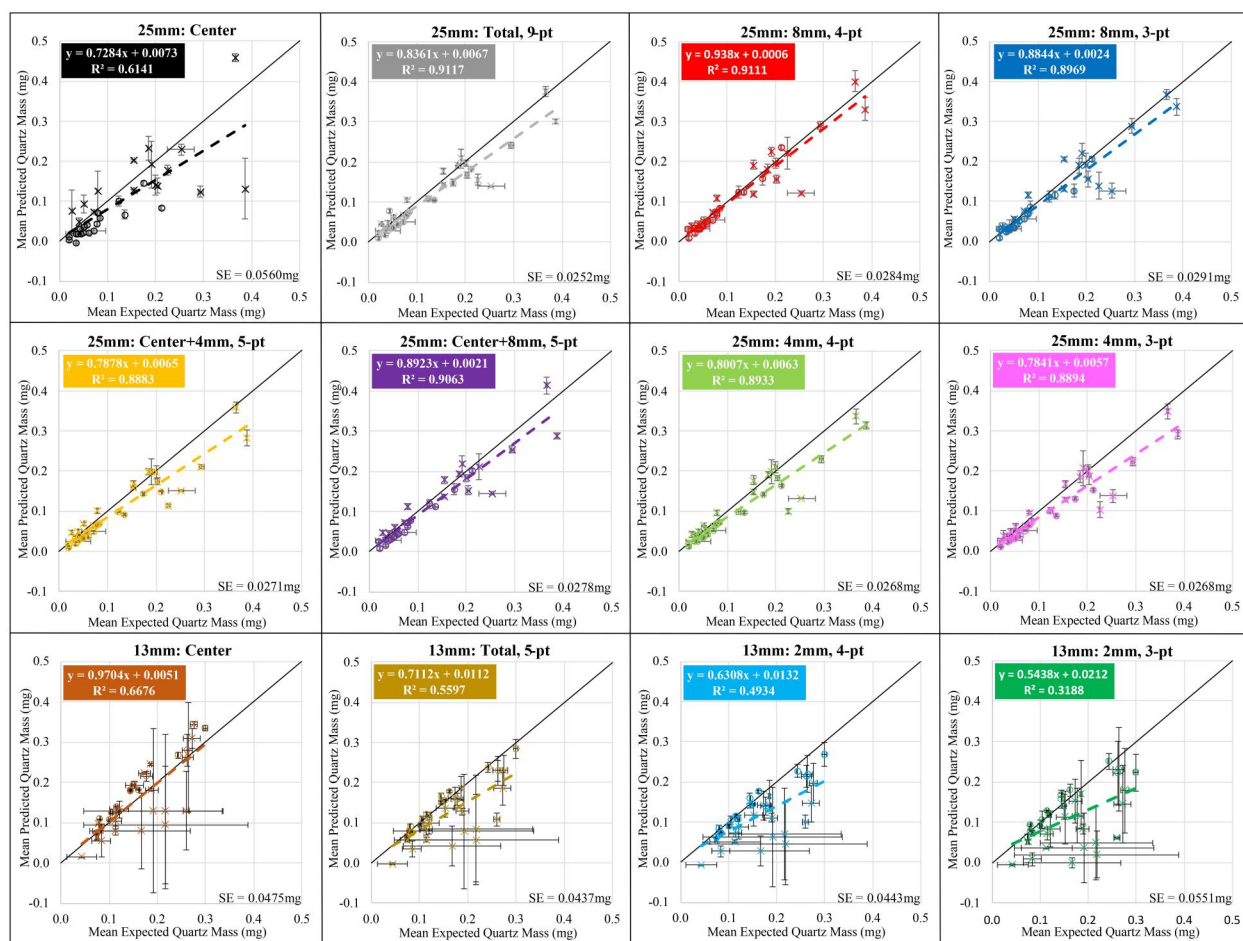


Figure 5. Correlation plots of mean predicted quartz mass vs. mean expected quartz mass for filters with dust deposited from mine source materials. The top two rows show the eight data combinations considered for 25-mm filters ($n = 35$), and the bottom row shows the four combinations considered for 13-mm filters ($n = 35$). Roof rock and bolter dust mine source materials are represented by the \times and data points, respectively.

consistent with expectations based on trends shown in Figure 3 and supported by SE analysis (values annotated on each plot). For all patterns other than “Center,” SE values were similar (between about 0.025 to 0.029 mg), regardless of whether the predicted quartz mass equation included a y-intercept value; however, the use of the equation with no y-intercept avoids prediction of negative values (i.e., so long as the combined QPA is positive). That said, the “8-mm, 4-pt” model can be considered superior based on its relative slope, which indicates that, on average, this model should predict about 94% of the expected quartz mass across the range of values studied here (i.e., approximately 0.020 to 0.400 mg, which corresponds to a total sample mass range of approximately 0.200 to 4.00 mg). Further, visual inspection of the plots for this model reveals that most scatter is due to higher mass samples. If, for example, only samples with expected quartz masses below 0.150 mg are considered (i.e., which equates to a total sample mass of

about 1.5 mg based on the quartz content of the coal mine source materials used here), the SE is just 0.011 mg.

Notably, Figure 5 shows that the regression line slopes are all substantially less than 1.0 for the model predictions including the center and/or 4-mm offset locations. This is attributed to the influence of high-mass samples, which are effectively pulling the trend-lines down. (This is likely due to gradual changes in the deposition pattern that occur with very high loading and is not expected to be related to the specific dust source material.) For the intended application (i.e., to analyze dust-recovered CPDM samples), the low to moderate range of total sample masses represented here is probably the most relevant (e.g., 0.200–1.500 mg). Nevertheless, the models relying on 8-mm offset data might be applicable across a very wide range of sample masses.

Concerning the 13-mm filters, Figure 5 (and Supplementary material, Figure S2) shows the model

using only the center-point data is most favorable, however, the SE values for all four models are higher than those observed for the 25-mm filter models (except the center-point model). This is attributed to substantial sample loss from some of the 13-mm filters; the associated data points are those that fall well below the plotted trendlines in [Figure 5](#). (It is noted that most of the filters that lost mass happened to have dust deposited from the roof rock source material, but susceptibility to sample loss is expected to depend more on total sample mass than on the dust source.) For these filters, there was generally also a large variation in the event-to-event QPA values, and hence predicted quartz mass values. Regardless, the susceptibility for sample loss probably makes the 13-mm filters an unfavorable choice moving forward—at least for moderate and high mass samples using the SS in-line syringe filter holder tested here. Interestingly, while the data from [Figure 3](#) hints that dust deposition might be center-heavy on the 13-mm filters, [Figure 5](#) shows that this pattern is exaggerated with higher total sample mass (i.e., compare the change in slope from “center” only to “2-mm” only plots in [Figure 5](#) vs. [Figure 3](#)).

Study implications and limitations

To the ultimate objective of enabling quartz analysis of CPDM samples collected in coal mines, the results of this study indicate that quartz mass could be accurately predicted by FTIR on a redeposited sample under specific conditions. Of the conditions considered here, deposition from an IPA suspension onto 25-mm PVC filters using a PP inline syringe filter holder was found to be more favorable than deposition onto 13-mm filters using an SS filter holder. This is related to two primary factors, namely the predictable “wheel and spoke” loading pattern yielded by the filter support included in the PP holder apparatus, and the relatively low susceptibility of the loaded filters to sample loss. Additionally, FTIR analysis of the loaded 25-mm filters with scans at four 8-mm center-offset locations (90° apart) yielded the most accurate quartz predictions. As stated, SE was just 11 µg for samples with a total mass less than about 1.5 mg, although SE more than doubled when considering the entire range of total sample mass studied here. The LOD and LOQ were estimated to be 5 µg and LOQ of 18 µg, respectively, per [Table S6](#) ([Supplementary material](#)). These values are consistent with those reported in previous studies of direct-on-filter FTIR analysis of traditional respirable coal mine dust

samples (i.e., collected with CMDPSUs) (Cauda et al. [2016](#), [2018](#); Hart et al. [2018](#))—and *could* be sufficient to inform non-regulatory RCS monitoring efforts. For context, assuming an 8-hr shift and standard 2.2 L/min flowrate for the CPDM, quartz masses of 53 µg and 26 µg would equate to the 50 µg/m³ PEL and 25 µg/m³ action level, respectively, set by the “new silica rule” (MSHA [2024](#)).

It is important to note that, for coal mines, the “new silica rule” requires standard quartz analysis of traditional RCMD filter samples in a certified lab (e.g., by MSHA Method P-7 or NIOSH Method 7603) (MSHA [2024](#)). Thus, analysis of recovered CPDM samples (at present) could not be used for regulatory purposes. However, given the relatively frequent CPDM sampling that is—and will continue to be—required to demonstrate compliance with RCMD exposure limits, capabilities to leverage these samples for additional RCS data could be very valuable. For instance, insights could be gained by tracking trends in quartz concentrations with specific worker activities and positioning, as well as geologic and mining conditions. The data derived from CPDM samples could provide added confidence that RCS overexposures are not occurring between the less frequent regulatory sampling for quartz.

Of course, all the above assumes that CPDM samples can be efficiently recovered (e.g., into IPA)—and that any interference from the CPDM filter stub materials can be accounted for. These points should be the focus of the next steps toward establishing a standardized method for quartz analysis of CPDM samples. To that end, further consideration of smaller-diameter filters for redeposition of the recovered CPDM sample might be prudent. In the current study, the 13-mm filters proved to be less favorable than the 25-mm filters, but this finding is related to both the sample masses and the filter support structure used here. For relatively small sample masses—which could be related to either the original CPDM sample or inefficient recovery of that sample—smaller redeposition filters could enable lower LOD and LOQ (based on quartz mass) since the dust will be more concentrated (e.g., see LOD/LOQ values in [Supplementary material, Table S6](#)). In that case, it might also be worthwhile to experiment with filter support like the “wheel and spoke” support used here with the 25-mm filters.

In terms of other study limitations, several should be acknowledged. First, while the IPA used to create the dust suspensions used here is not expected to interfere with the FTIR analysis of deposited dust, no attempt was made to confirm this point. Future

experiments could consider “procedural blanks” to account for both the IPA and blank PVC filter media—and even any residue recovered from the CPDM filter stub itself. Second, only a limited number of the samples generated for this work fell on the lower end of the quartz mass range that could be encountered when working with real CPDM samples. As mentioned, a quartz mass of just 26 µg for an 8-hr CPDM sample would represent the new 25 µg/m³ action level, so further evaluation of analytical accuracy at and below this level is important. It is worth noting that the design of such experiments requires attention to both the quartz mass and total sample mass ranges of interest. Here, MIN-U-SIL 5 material was used to establish the QPA-to-quartz mass calibration models because this material is well characterized and is nearly pure quartz; however, real RCMD samples will have a wide range of quartz contents. By coincidence, both coal mine source materials used to test the calibration models in this study had similar quartz contents (i.e., around 10%)—but it may be prudent to test on samples generated from additional materials with differing quartz contents, as well as on field samples.

Finally, it is acknowledged that this study relied on *expected* quartz mass to evaluate FTIR-predicted quartz mass. This approach assumes that the determination of quartz content (%) in each dust source material (i.e., by NIOSH Method 7603 and gravimetric analysis of a limited number of samples) was without error and that the materials were homogeneous such that all generated dust samples should have identical quartz content. The results do not suggest that these assumptions had any meaningful impact on study outcomes. An alternative approach would have been to analyze each dust sample generated for the study ($n = 30$ for MIN-U-SIL 5, $n = 35$ for coal mine source materials) by NIOSH Method 7603 following the analysis by FTIR. While that per-sample approach may eventually be necessary for evaluating FTIR-predicted quartz mass values on CPDM samples collected in the field (or otherwise generated from uncharacterized dust), it was cost-prohibitive for this study.

Conclusions

The continuous personal dust monitor (CPDM) is used for frequent measurement of respirable dust concentrations in coal mines. However, at present, there is no means by which to leverage the physical sample collected by the CPDM for analysis of crystalline silica (i.e., the most hazardous component of the dust).

Presuming that the CPDM sample could be recovered into a liquid suspension, this study demonstrates how the dust could be redeposited onto a clean PVC filter using a typical syringe filter apparatus—and then analyzed by FTIR. To accurately predict quartz mass (i.e., a proxy for crystalline silica in coal mine dust), results indicate that a multi-point scanning pattern is favorable when the “wheel and spoke” filter support is used; a single center-point scan might be sufficient if mesh support is used. In either case, the selection of filter size must consider the total anticipated sample mass to account for the required limits of detection and quantification, and minimize the potential for sample loss (i.e., due to caking). To fully develop a method for quartz analysis of CPDM samples by FTIR, the next steps should be to establish a sample recovery procedure—and quantify typical recovery (i.e., as a percentage of the total CPDM sample mass)—and any necessary corrections for analytical interference contributed by the CPDM filter stub itself.

Acknowledgments

We appreciate the support of our industry partners who facilitated site access for the collection of the coal mine source materials used in this study. Thanks also to Garek Elie for his support in developing the FTIR analysis cassette used in this study.

Disclosure statement

No potential conflict of interest was reported by the author(s).

Funding

This work was funded by the National Institute for Occupational Safety and Health (NIOSH) [contract 75D30119C05529].

Data availability statement

The authors confirm that the data supporting the findings of this study are available within the article and its supplementary materials.

References

- Ainsworth M. 2005. Infrared analysis of respirable coal mine dust for quartz: thirty-five years. *J ASTM Int.* 2(4): 12231. doi: [10.1520/JAI12231](https://doi.org/10.1520/JAI12231).
- Blackley DJ, Crum JB, Halldin CN, Storey E, Laney AS. 2016. Resurgence of progressive massive fibrosis in coal

- miners—Eastern Kentucky, 2016. *MMWR Morb Mortal Wkly Rep.* 65(49):1385–1389. doi: [10.15585/mmwr.mm6549a1](https://doi.org/10.15585/mmwr.mm6549a1).
- Blackley DJ, Halldin CN, Laney AS. 2018. Continued increase in prevalence of coal workers' pneumoconiosis in the United States, 1970–2017. *Am J Public Health.* 108(9):1220–1222. doi: [10.2105/AJPH.2018.304517](https://doi.org/10.2105/AJPH.2018.304517).
- Cantrell BK, Stein SW, Patashnick H, Hassel D. 1996. Status of a tapered element, oscillating microbalance-based continuous respirable coal mine dust monitor. *Appl Occup Environ Hyg.* 11(7):624–629. doi: [10.1080/1047322X.1996.10389950](https://doi.org/10.1080/1047322X.1996.10389950).
- Castranova V, Vallyathan V. 2000. Silicosis and coal workers' pneumoconiosis. *Environ Health Perspectives.* 108(4):675–684.
- Cauda E, Chubb L, Reed R, Stepp R. 2018. Evaluating the use of a field-based silica monitoring approach with dust from copper mines. *J Occup Environ Hyg.* 15(10):732–742. doi: [10.1080/15459624.2018.1495333](https://doi.org/10.1080/15459624.2018.1495333).
- Cauda E, Drake P, Lee T, Pretorius C. 2014. High-volume samplers for the assessment of respirable silica content in metal mine dust via direct-on-filter analysis. In: *Proceedings of the Tenth International Mine Ventilation Congress*; 2–8 August; Sun City, Northwest Province, South Africa.
- Cauda E, Miller A, Drake P. 2016. Promoting early exposure monitoring for respirable crystalline silica: taking the laboratory to the mine site. *J Occup Environ Hyg.* 13(3):D39–D45. doi: [10.1080/15459624.2015.1116691](https://doi.org/10.1080/15459624.2015.1116691).
- Chien CH, Huang G, Lopez B, Morea A, Sing SY, Wu CY, Kashon ML, Harper M. 2020. Application of end-of-shift respirable crystalline silica monitoring to construction. *J Occup Environ Hyg.* 17(9):416–425. doi: [10.1080/15459624.2020.1779275](https://doi.org/10.1080/15459624.2020.1779275).
- Chow JC, Watson JG, Wang X, Abbasi B, Reed WR, Parks D. 2022. Review of filters for air sampling and chemical analysis in mining workplaces. *Minerals.* 12(10):1314. doi: [10.3390/min12101314](https://doi.org/10.3390/min12101314).
- Cohen RA, Rose CS, Go L, Zell-Baran L, Almberg KS, Sarver E, Lowers H, Iwaniuk C, Clingerman S, Richardson D, et al. 2022. Increased silica burden is associated with pathologic features of alveolar proteinosis, mature and immature silicotic nodules in US coal miners with progressive massive fibrosis (PMF). In: *B25. Advances in Occupational Lung Disease*; San Francisco (CA). p. A2492. doi: [10.1164/ajrccm-conference.2022.205.1_MeetingAbstracts.A2492](https://doi.org/10.1164/ajrccm-conference.2022.205.1_MeetingAbstracts.A2492).
- Farcas D, Lee T, Chisholm WP, Soo JC, Harper M. 2016. Replacement of filters for respirable quartz measurement in coal mine dust by infrared spectroscopy. *J Occup Environ Hyg.* 13(2):D16–D22. doi: [10.1080/15459624.2015.1091962](https://doi.org/10.1080/15459624.2015.1091962).
- Goldberg S, Tomb T, Kacsmar P, Baber J, Busa M. 1984. MSHA's procedure for determining quartz content of respirable coal mine dust. Informational Report. Pittsburgh (PA): Mine Safety and Health Administration, U.S. Department of Labor. Report No.: IR 1152.
- Greth A, Afrouz S, Animah F, Keles C, Sarver E. 2023. Recovery of respirable dust from fibrous filters for particle analysis by scanning electron microscopy. Paper presented at: the 19th North American Mine Ventilation Symposium; Rapid City, SD. doi: [10.1201/9781003429241-24](https://doi.org/10.1201/9781003429241-24).
- Greth A, Afrouz SG, Keles C, Sarver E. 2024. Characterization of respirable coal mine dust recovered from fibrous polyvinyl chloride filters by scanning electron microscopy. *Mining Metall. Explor.* 41(3):1145–1154. doi: [10.1007/s42461-024-00999-z](https://doi.org/10.1007/s42461-024-00999-z).
- Hall NB, Blackley DJ, Halldin CN, Laney AS. 2019a. Current review of pneumoconiosis among US coal miners. *Curr Environ Health Rep.* 6(3):137–147. doi: [10.1007/s40572-019-00237-5](https://doi.org/10.1007/s40572-019-00237-5).
- Hall NB, Blackley DJ, Halldin CN, Laney AS. 2019b. Continued increase in prevalence of r-type opacities among underground coal miners in the USA. *Occup Environ Med.* 76(7):479–481. doi: [10.1136/oemed-2019-105691](https://doi.org/10.1136/oemed-2019-105691).
- Hart JF, Autenrieth DA, Cauda E, Chubb L, Spear TM, Wock S, Rosenthal S. 2018. A comparison of respirable crystalline silica concentration measurements using a direct-on-filter Fourier transform infrared (FT-IR) transmission method vs. a traditional laboratory X-ray diffraction method. *J Occup Environ Hyg.* 15(10):743–754. doi: [10.1080/15459624.2018.1495334](https://doi.org/10.1080/15459624.2018.1495334).
- Jacobson M, Lamonica J. 1969. Personal respirable dust sampler. Washington (DC): Department of the Interior (US). Technical Progress Report 17 Sept 1969.
- Key-Schwartz RJ, Baron PA, Bartley DL, Rice FL, Schlecht PC. 2003. Chapter R, Determination of airborne crystalline silica. In: *NIOSH manual of analytical methods*. 4th ed., 3rd Suppl. Cincinnati (OH): U.S. Department of Health and Human Services, Public Health Service, Centers for Disease Control and Prevention, National Institute for Occupational Safety and Health, DHHS (NIOSH) Publication No. 2003–154.
- Kissell F, Volkwein J, Kohler J. 2002. Historical perspective of personal dust sampling in coal mines. Paper presented at: The North American Mine Ventilation Symposium, Kingston, Canada.
- Laney AS, Weissman DN. 2014. Respiratory diseases caused by coal mine dust. *J Occup Environ Med.* 56 Suppl 10(10):S18–S22. doi: [10.1097/JOM.0000000000000260](https://doi.org/10.1097/JOM.0000000000000260).
- Liu T, Liu S. 2020. The impacts of coal dust on miners' health: a review. *Environ Res.* 190:109849. doi: [10.1016/j.envres.2020.109849](https://doi.org/10.1016/j.envres.2020.109849).
- Lorberau C. 1990. Technical brief: investigation of the determination of respirable quartz on filter media using Fourier transform infrared spectrophotometry. *Appl Occup Environ Hyg.* 5(6):348–350. doi: [10.1080/1047322X.1990.10389652](https://doi.org/10.1080/1047322X.1990.10389652).
- Miller AL, Drake PL, Murphy NC, Cauda EG, LeBouf RF, Markevicius G. 2013. Deposition uniformity of coal dust on filters and its effect on the accuracy of FTIR analyses for silica. *Aerosol Sci Technol.* 47(7):724–733. doi: [10.1080/02786826.2013.787157](https://doi.org/10.1080/02786826.2013.787157).
- Miller AL, Drake PL, Murphy NC, Noll JD, Volkwein JC. 2012. Evaluating portable infrared spectrometers for measuring the silica content of coal dust. *J Environ Monit.* 14(1):48–55. doi: [10.1039/c1em10678c](https://doi.org/10.1039/c1em10678c).
- Miller AL, Murphy NC, Bayman SJ, Briggs ZP, Kilpatrick AD, Quinn CA, Wadas MR, Cauda EG, Griffiths PR. 2015. Evaluation of diffuse reflection infrared spectrometry for end-of-shift measurement of quartz in coal dust

- samples. *J Occup Environ Hyg.* 12(7):421–430. doi: [10.1080/15459624.2015.1011328](https://doi.org/10.1080/15459624.2015.1011328).
- Miller AL, Weakley AT, Griffiths PR, Cauda EG, Bayman S. 2017. Direct-on-filter alpha-quartz estimation in respirable coal mine dust using transmission fourier transform infrared spectrometry and partial least squares regression. *Appl Spectrosc.* 71(5):1014–1024. doi: [10.1177/0003702816666288](https://doi.org/10.1177/0003702816666288).
- [MSHA] Mine Safety and Health Administration. 1994. Infrared determination of quartz in respirable coal mine dust: Method P-7. Pittsburgh (PA): U.S. Department of Labor, Mine Safety and Health Administration.
- [MSHA] Mine Safety and Health Administration. 2014. Lowering miners' exposure to respirable coal mine dust, including continuous personal dust monitors. United States, Department of Labor. Document No.: 79 FR 24814.
- [MSHA] Mine Safety and Health Administration. 2024. Lowering miners' exposure to respirable crystalline silica and improving respiratory protection. United States, Department of Labor. Document No.: 89 FR 44852.
- [NASEM] National Academies of Sciences, Engineering, and Medicine. 2018. Monitoring and sampling approaches to assess underground coal mine dust exposures. Washington (DC): The National Academies Press. doi: [10.17226/25111](https://doi.org/10.17226/25111).
- [NIOSH] National Institute for Occupational Safety and Health. 2003. Quartz in coal mine dust, by IR: Method 7603. In: Schlecht PC, O'Connor PF, editors. *NIOSH manual of analytical methods*. 4th ed. Cincinnati (OH): U.S. Department of Health and Human Services, Publication No. 94–113.
- [NIOSH] National Institute for Occupational Safety and Health. 2011. Coal mine dust exposures and associated health outcomes. *Current Intelligence Bulletin* 64. U.S. Department of Health and Human Services, Publication No.: 2011–172..
- [NIOSH] National Institute for Occupational Safety and Health. 2022. Direct-on-filter analysis for respirable crystalline silica using a portable FTIR instrument. Pittsburgh (PA): U.S. Department of Health and Human Services, Centers for Disease Control and Prevention, National Institute for Occupational Safety and Health. Report No.: 2022–108, IC 9533. doi: [10.26616/NIOSH PUB2022108](https://doi.org/10.26616/NIOSH PUB2022108).
- Ojima J. 2003. Determining of crystalline silica in respirable dust samples by infrared spectrophotometry in the presence of interferences. *J Occup Health.* 45(2):94–103. doi: [10.1539/joh.45.94](https://doi.org/10.1539/joh.45.94).
- Osho B, Elahifard M, Wang X, Abbasi B, Chow JC, Watson JG, Arnott WP, Reed WR, Parks D. 2024. Evaluation of PVC and PTFE filters for direct-on-filter crystalline silica quantification by FTIR. *J Occup Environ Hyg.* 21(8):539–550. doi: [10.1080/15459624.2024.2357080](https://doi.org/10.1080/15459624.2024.2357080).
- Page SJ, Tuchman DP, Vinson RP. 2007. Thermally induced filter bias in TEOM mass measurement. *J Environ Monit.* 9(7):760–767. doi: [10.1039/b704424k](https://doi.org/10.1039/b704424k).
- Pampena JD, Cauda EG, Chubb LG, Meadows JJ. 2020. Use of the field-based silica monitoring technique in a coal mine: a case study. *Min Metall Explor.* 37(2):717–726. doi: [10.1007/s42461-019-00161-0](https://doi.org/10.1007/s42461-019-00161-0).
- Pokhrel N, Agioutanti E, Keles C, Afrouz S, Sarver E. 2022. Comparison of respirable coal mine dust constituents estimated using FTIR, TGA, and SEM–EDX. *Mining Metall Explor.* 39(2):291–300. doi: [10.1007/s42461-022-00567-3](https://doi.org/10.1007/s42461-022-00567-3).
- Pokhrel N, Keles C, Jaramillo L, Agioutanti E, Sarver E. 2021. Direct-on-filter FTIR spectroscopy to estimate calcite as a proxy for limestone 'rock dust' in respirable coal mine dust samples. *Minerals.* 11(9):922. doi: [10.3390/min11090922](https://doi.org/10.3390/min11090922).
- Schatzel SJ. 2009. Identifying sources of respirable quartz and silica dust in underground coal mines in southern West Virginia, western Virginia, and eastern Kentucky. *Int J Coal Geol.* 78(2):110–118. doi: [10.1016/j.coal.2009.01.003](https://doi.org/10.1016/j.coal.2009.01.003).
- Stacey P, Clegg F, Rhyder G, Sammon C. 2022. Application of a Fourier transform infrared (FTIR) principal component regression (PCR) chemometric method for the quantification of respirable crystalline silica (quartz), kaolinite, and coal in coal mine dusts from Australia, UK, and South Africa. *Ann Work Expo Health.* 66(6):781–793. doi: [10.1093/annweh/wxab119](https://doi.org/10.1093/annweh/wxab119).
- Stacey P, Kauffer E, Moulut JC, Dion C, Beauparlant M, Fernandez P, Key-Schwartz R, Friede B, Wake D. 2009. An international comparison of the crystallinity of calibration materials for the analysis of respirable α -quartz using X-ray diffraction and a comparison with results from the infrared KBr disc method. *Ann Occup Hyg.* 53(6):639–649. doi: [10.1093/annhyg/mep038](https://doi.org/10.1093/annhyg/mep038).
- Su X, Ding R, Zhuang X. 2020. Characteristics of dust in coal mines in Central North China and its research significance. *ACS Omega.* 5(16):9233–9250. doi: [10.1021/acsomega.0c00078](https://doi.org/10.1021/acsomega.0c00078).
- Tuchman DP, Volkwein JC, Vinson RP. 2008. Implementing infrared determination of quartz particulates on novel filters for a prototype dust monitor. *J Environ Monit.* 10(5):671–678. doi: [10.1039/b803804j](https://doi.org/10.1039/b803804j).
- Weakley AT, Miller AL, Griffiths PR, Bayman SJ. 2014. Quantifying silica in filter-deposited mine dusts using infrared spectra and partial least squares regression. *Anal Bioanal Chem.* 406(19):4715–4724. doi: [10.1007/s00216-014-7856-y](https://doi.org/10.1007/s00216-014-7856-y).
- Williams KL, Vinson RP. 1986. Evaluation of TEOM dust monitor. Pittsburgh (PA): US Department of the Interior, Bureau of Mines. p. 9119.
- Volkwein JC. 2008. Analysis of particulate contamination in personal dust monitor sampling. Paper presented at: the 12th North American Mine Ventilation Symposium; Reno, NV.
- Volkwein JC, Thimons ED, Timko RJ, Hall EE, Mischler SE, Kissell FN, Vinson RP. 2005. State-of-the-art in monitoring respirable mine aerosols. Paper presented at: the 8th International Mine Ventilation Congress; Brisbane, Australia.
- Volkwein JC, Tuchman DP, Vinson RP. 2002. Performance of a prototype personal dust monitor for coal mine use. Paper presented at: The North American Mine Ventilation Symposium; Kingston, Canada.
- Volkwein JC, Vinson RP, McWilliams LJ, Tuchman DP, Mischler SE. 2004. Performance of a new personal respirable dust monitor for mine use. Pittsburgh (PA): U.S. Department of Health and Human Services, Report of Investigations 9663.
- Volkwein JC, Vinson RP, Page SJ, McWilliams LJ, Joy GJ, Mischler SE, Tuchman DP. 2006. Laboratory and field performance of a continuously measuring personal respirable dust monitor. Pittsburgh (PA): U.S. Department of Health and Human Services, Report of Investigations 9669.